

December 2023

## Reducing Scour Hole Dimensions around Bridge Circular Piers Using Hexagonal Collars

Heba Kassem

*Irrigation and Hydraulics Engineering Department, Faculty of Engineering, Mansoura University, Egypt, safe15402@gmail.com*

El-Masry A. A

*Irrigation and Hydraulics Engineering Department, Faculty of Engineering, Mansoura University, Egypt*

Reda Diab

*Irrigation and Hydraulics Engineering Department, Faculty of Engineering, Mansoura University, Egypt*

Follow this and additional works at: <https://mej.researchcommons.org/home>



Part of the [Architecture Commons](#), and the [Engineering Commons](#)

---

### Recommended Citation

Kassem, Heba; A, El-Masry A.; and Diab, Reda (2023) "Reducing Scour Hole Dimensions around Bridge Circular Piers Using Hexagonal Collars," *Mansoura Engineering Journal*: Vol. 48 : Iss. 4 , Article 11. Available at: <https://doi.org/10.58491/2735-4202.3087>

This Original Study is brought to you for free and open access by Mansoura Engineering Journal. It has been accepted for inclusion in Mansoura Engineering Journal by an authorized editor of Mansoura Engineering Journal. For more information, please contact [mej@mans.edu.eg](mailto:mej@mans.edu.eg).

## ORIGINAL STUDY

# Reducing Scour Hole Dimensions Around Bridge Circular Piers Using Hexagonal Collars

Heba Kassem\*, Adel El-Masry, Reda Diab

Irrigation and Hydraulics Engineering Department, Faculty of Engineering, Mansoura University, Egypt

### Abstract

Bridge failure, due to local scour at bridge circular pier foundations, has become a critical issue in river and bridge engineering, which might lead to transportation disruption, loss of lives and economic problems. Based on an experimental perspective, this study is focused on the influence of collar's shape on decreasing scour depth at bridge piers that were explored. Hexagonal collars with three shapes were investigated (sloped, sloped with holes, and sloped with ribs). The collars were installed on the bed level with diameter equals to three times the diameter of pier. To achieve the results, experiments were performed in clear-water conditions using uniform sand for bed materials. Results indicated that all types of collars provide a considerable decrease in the scour depth and delayed the formation of scouring holes. Sloped with ribs hexagonal collar appeared to be the most effective collar shape in reducing scour around the pier by 56% reduction in the scour depth, while the upstream length, downstream length, and the width of the scour are reduced by 29%, 51%, and 19% respectively compared with the case of the pier without collars. Empirical dimensionless relations for maximum scour depth, width, and length are generated according to the experimental results.

**Keywords:** Bridge piers, Clear-water scour, Countermeasures, Experimental work, Hexagonal collar

## 1. Introduction

Scour was defined as a natural phenomenon created by a river flow of water. It formed as a result of the actions of moving water, which dissolves and erodes material from riverbeds and banks, as well as the region around bridge piers, Breusers et al. (1977), Melville and Coleman (Melville and Coleman, 2000), and Richardson and Davis (2001) distinguished two forms of scour: general scour and localized scour. Due to the difficulty in identifying the nature of complex flow and the system of scouring that is responsible for bridge failure problem in many nations around the world, it was crucial to investigate scour across bridge piers to know how to limit and predict scour and prevent bridge failures. Scholars had worked hard to reduce the size of scour holes around the piers using a variety of scour countermeasures. Tafarojnoruz et al. (2010) divided the countermeasures into two cases: armoring methods and flow-altering

methods. The collar was one of the piers' flow-altering countermeasures by providing a sediment layer and a mechanism that avoids contact with the horseshoe-shaped vortex leading to protecting soil particles against erosion via a downstream direct effect. There are many studies revealed the effect of collars on the scour depth. Helmi et al. (2019) found that wider collar installed at a lower elevation relative to the bed surface is more effective. The impact of the collar on the circular pier had been the subject of several researches including Bestawy et al. (2020) who examined the effectiveness of several circular collars around the piers and discovered that the conical collar was the most effective in lowering scour around the bridge pier with a 61.1% reduction in scour depth downstream of the pier.

Safaei et al. (2021) suggested the case of flexible and permeable collar. The technique is given in the form of a flexible chain collar three times the diameter of the pier. Three distinct chain diameters were used to control the influence of chain shapes.

Received 23 April 2023; revised 9 August 2023; accepted 18 August 2023.  
Available online 15 December 2023

\* Corresponding author.  
E-mail address: safe15402@gmail.com (H. Kassem).

<https://doi.org/10.58491/2735-4202.3087>

2735-4202/© 2023 Faculty of Engineering, Mansoura University. This is an open access article under the CC BY 4.0 license (<https://creativecommons.org/licenses/by/4.0/>).

Results showed that the scour depth reduced with increasing the diameter of chain ring. [Raeisi and Ghomeshi \(2022\)](#) studied the influence of collar shape on lowering scour depth. Collars were tested in two asymmetrical oval shapes at three different levels. The results revealed that collars installed on the bed surface with the largest diameter revealed great result in controlling scour. [Pandey et al. \(2020\)](#) noted that the efficacy of a symmetrical collar in minimizing scour holes around a circular bridge's pier. According to their investigation, employing the collar minimizes the maximum scour around the pier by almost 60% when compared to the results without collar. [Gupta et al. \(2023\)](#) investigated the airfoil shape of collar as scour countermeasure around the pier. Results indicated that the collar diameter is increased; the scour depth around the pier is reduced. Installing the airfoil collar shape at the bed improves the collar performance and no scour was observed around pier.

[Negm et al. \(2009\)](#) suggested different shapes of collars (triangular, circular, trapezoidal, and rectangular) to reduce the scour depth around the pier. The use of the rectangular collar shape decrease the maximum scour depth around the bridge pier to the extent of 90% compared with the pier without collar. [Moncada-M et al. \(Moncada et al., 2009\)](#) studied the effect of the different sizes and the locations of collar around circular pier, it was founded that, when the collar was placed at the bed level, the minimum scour depth was reached. The scour depth is reduced when the diameter is increased. Furthermore, their research demonstrated that the collar's efficiency reduced with the height of crown installation on the bridge pier that grows near the

sedimentary surface of the bed. According to an analysis of relevant literature, many studies assessed scour behavior around specific layout of collar, but there is no research concentrated on making a contrast of those types and with an accent on the critical roles of collar design on the scour around pier protection. Therefore, this research aims to investigate the impact of novel collar shapes on the dimensions of the scour hole at a circular pier.

## 2. Dimensional analysis

Several independent parameters including pier structures' parameters, flow specifications, sediment characteristics, cross-section geometry, and anti-scour device features influence the geometry of a scour hole around the bridge piers. The dependent dimensions of a scour hole can be related to the essential independent parameters as following mathematical function, [Fig. 1](#):

$$L = f(h, V, V_{cr}, \rho, g, \nu, \rho_s, d_{50}, B, b, D, \sigma, K_m, T) \quad (1)$$

Where:  $L$  refers to the considered dimension of the scour hole, namely:  $d_s$  is the maximum scour depth (L),  $W_s$  is the maximum width of the scour hole (L), and  $L_u$  &  $L_d$  are the maximum upstream and downstream lengths of the scour hole (L), respectively.  $h$  is the water depth (L),  $V$  is the mean flow velocity (L/T),  $V_{cr}$  is the critical flow velocity (L/T),  $\rho$  is the water density (M/L<sup>3</sup>),  $g$  is the gravity acceleration (L/T<sup>2</sup>),  $\nu$  is the dynamic viscosity of the liquid (ML<sup>-1</sup>T<sup>-1</sup>),  $d_{50}$  is the mean particle sizes for which 50% of sediment finer (L). In addition,  $B$  is the flume width (L),  $b$  is the pier diameter (L),  $D$  is the

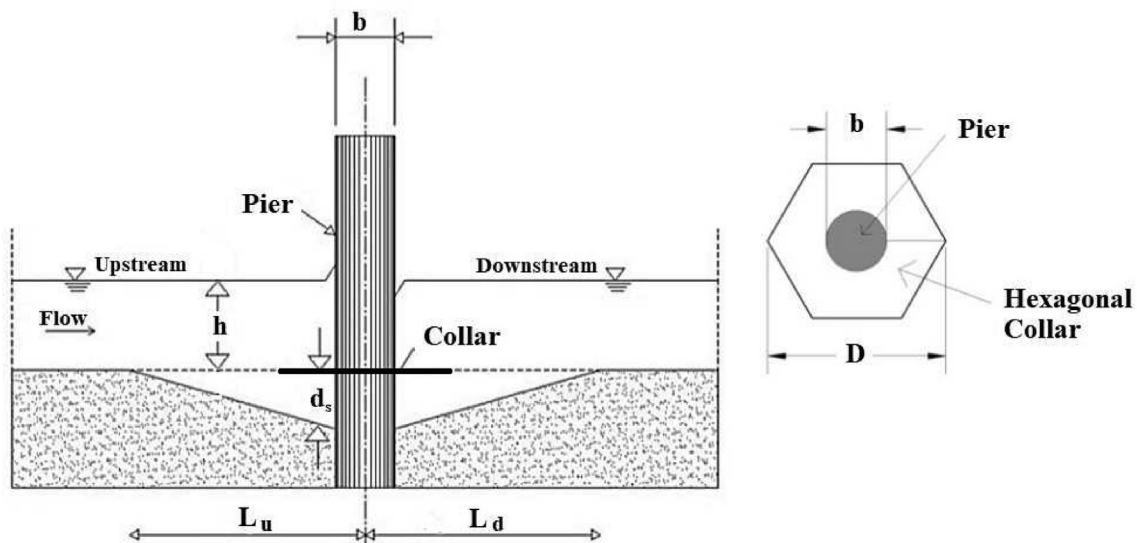


Fig. 1. Layout of local scour parameters.

collar diameter ( $L$ ),  $K_m$  is the coefficient of collar shape effect (–) and  $T$  is the equilibrium time of scour ( $T$ ).

The Buckingham dimensional analysis method is applied considering that no viscous effect and assuming  $b$ ,  $V$  and  $\rho$  as iterative variables. The relation between nondimensional dependent and independent scour parameters is expressed as:

$$\frac{d_s}{b}, \frac{W_s}{b}, \frac{L_u}{b} \text{ or } \frac{L_d}{b} = f \left( \frac{h}{b}, \frac{V}{V_{cr}}, F_r, \frac{b}{B}, \frac{b}{d_{50}}, \sigma, \frac{D}{b}, K_m \right) \quad (2)$$

Where:  $\frac{d_s}{b}$ ,  $\frac{W_s}{b}$ ,  $\frac{L_u}{b}$  or  $\frac{L_d}{b}$  are the nondimensional (relative) maximum depth, width, upstream and downstream lengths of the scour holes,  $\frac{h}{b}$  is the nondimensional (relative) water depth to pier diameter (flow shallowness). In addition  $\frac{V}{V_{cr}}$  is the mean to critical flow velocity ratio (flow intensity),  $F_r = V/\sqrt{g \cdot h}$  is Froude number,  $\frac{b}{B}$  is the relative pier diameter to canal width (contraction ratio),  $\frac{b}{d_{50}}$ ,  $\sigma$  are the sediment coarseness (the standard deviation of the bed material), respectively, and  $K_m$  is the novel coefficient of collar model effect.

This study focused on the impact of collar's shape expressed as the coefficient of collar model ( $K_m$ ) on local pier scour at equilibrium under different clear-water scour conditions. Therefore, some of the above-mentioned factors were set to be constant at the recommended values in the state-of-the-art including  $\left(\frac{b}{B}, \frac{b}{d_{50}}, \sigma, \frac{D}{b}\right)$ , and the collar was placed on the bed surface during all runs. From which and according to the study's goals, the effect of these

parameters is out of this study, and equation (2) can be rewritten for each scour dimension as:

$$\frac{d_s}{b} = f \left( \frac{h}{b}, \frac{V}{V_{cr}}, F_r, K_m \right) \quad (3)$$

$$\frac{W_s}{b} = f \left( \frac{h}{b}, \frac{V}{V_{cr}}, F_r, K_m \right) \quad (4)$$

$$\frac{L_u}{b} = f \left( \frac{h}{b}, \frac{V}{V_{cr}}, F_r, K_m \right) \quad (5)$$

$$\frac{L_d}{b} = f \left( \frac{h}{b}, \frac{V}{V_{cr}}, F_r, K_m \right) \quad (6)$$

### 3. Experimental work

#### 3.1. Experimental set-up

The experiments are carried out at the Irrigation and Hydraulics Laboratory of faculty of Engineering, Mansoura University (Egypt). Tests were performed in a recirculating current flume with the dimensions of 12 m long Perspex side wall, 77 cm wide and 60 cm depth, [Photo 1](#) and [Fig. 2](#). The required flow discharge deliveries from a ground water tank using two pumps through the 1.0 m × 1.0 m size inlet tank. After passing the 12 m main flume, the outflow occurs over a tailgate and through two tanks in series, the 1.0 m × 1.0 m size outlet tank and the weir control tank again to the ground tank. A flow control valve was used to



Photo 1. The experimental apparatus.

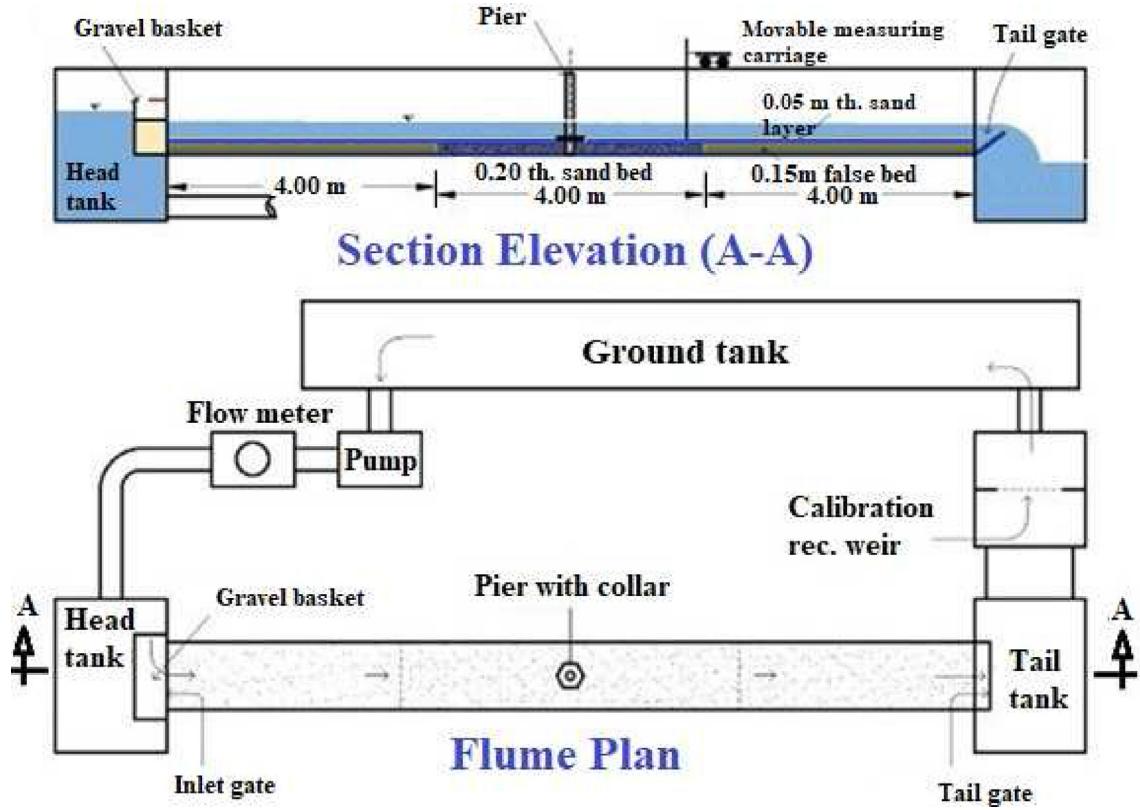


Fig. 2. Sketch of the used flume and the experimental set-up.

assure the pre-specified discharge rates. The tail water level can be adjusted by a tail gate. The discharge is measured using a controlled sharp rectangular weir. A digital point gauge mounted on

a movable measuring carriage was used to expose the scour hole.

The pier and collar models are installed in a 4.0 m long working section located in the middle of the

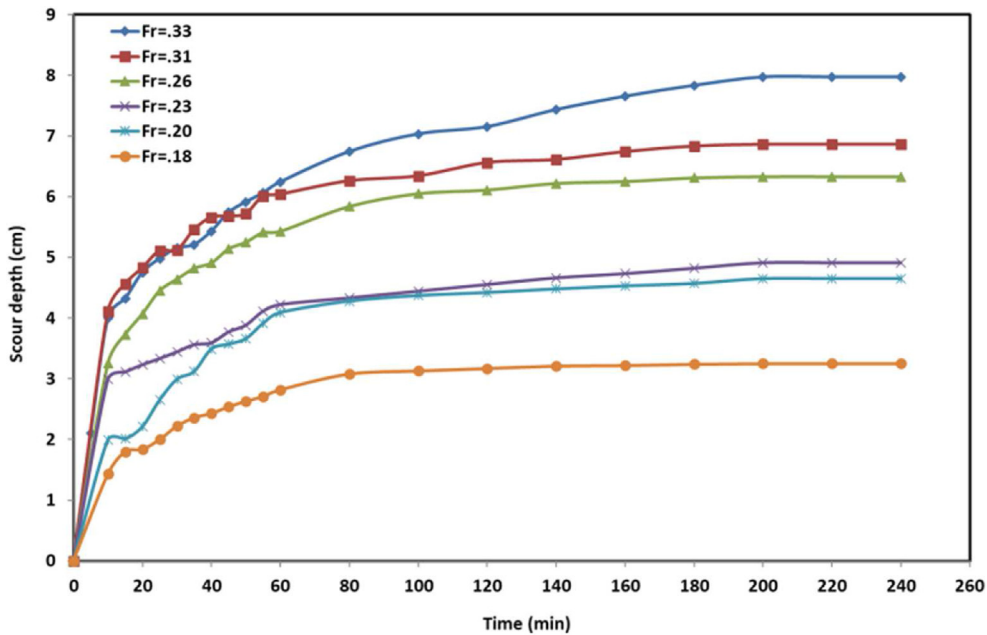


Fig. 3. Equilibrium time of scour depth.



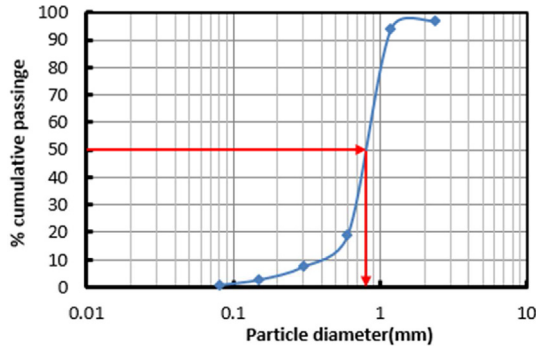


Fig. 4. Sieve analysis of bed material.

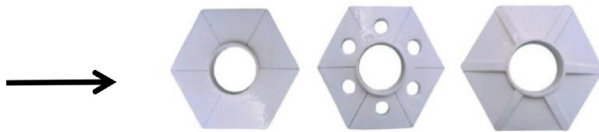


Photo 2. Considered collar's shapes.

flume and filled with 0.20 m thickness of uniform sand. The wooden false bed extended 4.0 m upstream and 4.0m downstream the work section with a constant thickness equal to 15.0 cm. The false bed was covered by sand layer of 5.0 cm thickness to unify the bed shear stress and boundary conditions. A basket filled with gravel was placed at the flume's inlet tank to laminarize the inflow. Perspex side walls make it easier to monitor and gauge flow and scour parameters.

The total number of conducted experiments is twenty-four runs. The tests are stopped after 4 h of running time until achieving the equilibrium stage when the rate of change in scour depth is less than

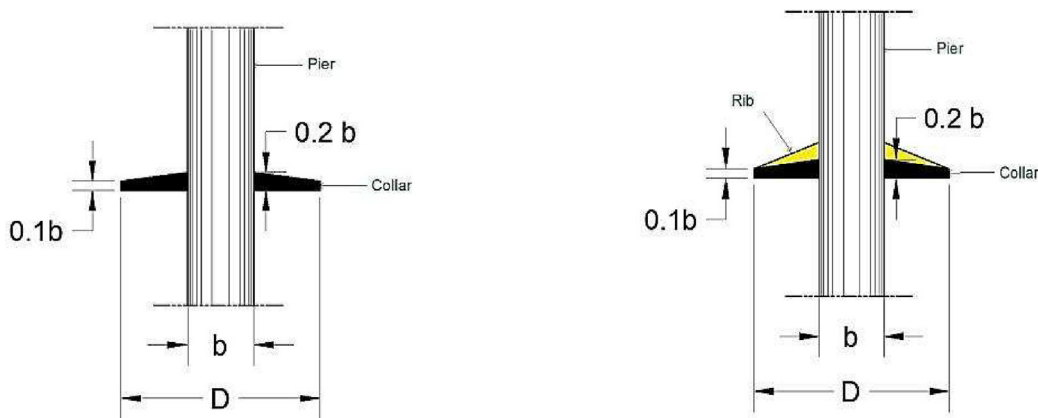
3% and the increasing in scour depth became lesser than 5% of the pier diameter according to (Diab et al., 2010; Melville and Chiew, 1999), respectively, as shown in Fig. 3.

### 3.2. Sediment material

Fig. 4 represents the sediment material used in all runs. The median grain size was  $d_{50} = 0.80$  mm and the geometric standard deviation  $\sigma = 1.44$ . The specific gravity of the used sand equals 2.65. The sediment material is considered uniform sand because of  $\sigma = 1.44 < 1.50$  as mentioned in the literatures (Chiew and Melville, 1987; Gumgum and Guney, 2020; Raudkivi and Ettema, 1983).

### 3.3. Pier and hexagonal collars

The pier was made of polyvinyl chloride (PVC) with a diameter of 6.0 cm. It was first fixed vertically in the flume at the center of the measuring section. In this study, three collar shapes were made of wood and painted with epoxy, Photo 2. Bestawy et al. (2020) suggested that a ratio of  $D/b \sim 3$  to 3.5 is the most effective size in scour reduction for a collar. In this study, the diameter of the collar is equal to  $D/b = 3$  and is placed on the bed surface. The hexagonal collar family formed as sloped, sloped with holes, and sloped with ribs. Sloped collars have a thickness equal to  $0.1b$  at the outer perimeter and  $0.2b$  at the inner perimeter. The ribs of collars are fixed on the upper surface with  $0.1b$  thickness and sloped height from  $0.1b$  to zero at the outer edge of the collar. The holes of the collars are  $0.33b$  in diameter where  $b$  is the diameter of the pier, Fig. 5.



a) Sloped hexagonal collar

b) Sloped with ribs hexagonal collar

Fig. 5. Considered details of sloped and sloped with ribs hexagonal collars.

Table 1. Flow characteristics.

Q (L/s)	h (cm)	V (m/sec)	$\frac{V}{V_{cr}}$	$F_r$ (-)
20.0	8.5	0.31	0.93	0.33
	9.0	0.29	0.87	0.31
	10.0	0.26	0.77	0.26
	11.0	0.24	0.69	0.23
	12.0	0.22	0.62	0.20
	13.0	0.20	0.57	0.18

### 3.4. Experimental procedures

To examine the impacts of a broad range of flow intensities and Froude numbers, six depths of flow for constant discharge were examined as indicated in Table 1. All experiments were conducted with the uniform sand bed under clear-water scour conditions. The critical flow velocity was calculated by equation (8) according to Chiew and Melville (Chiew and Melville, 1987).

$$u^*_{cr} = 0.0115 + 0.012d_{50}^{1.4}, 0.1 \text{ mm} < d < 1 \text{ mm} \quad (7)$$

$$\frac{V_c}{U^*_{cr}} = 5.75 \log \frac{h}{2d_{50}} + 6 \quad (8)$$

Where;  $U^*_{cr}$  is the critical shear velocity for the sediment.

Where:  $\frac{V}{V_{cr}} < 1$  is a clear-water condition to obtain the maximum scour depth not the equilibrium scour depth. The flow is subcritical and steady, which  $Fr < 1$  and Q is constant with time. The existence of

an obstructive object such as a bridge pier in a flow field leads to the generation of three-dimensional accelerating turbulent flow, and flow vortices, which entrain bed sediments in the vicinity of the pier.

The flume bed has been carefully leveled by using a scrapper to ensure surface regularities along the flume bed. For keeping standard measured level constant, point gauge and spirit level were used. The leveling should be checked before each experiment in random places. Water flow filled the flume slowly until the sand bed material was saturated, then the downstream gate was gradually adjusted to reach the required flow depth. Preliminary experiments were set-up to determine the experimental time duration, which is enough to reach equilibrium scour depths in which the increase of scour depth was observed to be negligible. For each experiment, after the anticipated run time, the pump valve was closed. Flow depth was allowed to drain from the flume to the sump at a slow rate. A digital point gauge was used to record scour depth for each run. It was taken into consideration using the same measurement tools to prevent any error that can occur. The difference between the final elevation and the datum reading (original bed) measures how much the bed scoured or filled.

## 4. Results and discussion

The conducted experiments were listed in Table 2. The relative dimensions of the considered values for

Table 2. The experimental results of the considered cases.

Fr	Pier without collar				Hexagonal											
	$d_s$ (cm)	$W_s$ (cm)	$L_u$ (cm)	$L_d$ (cm)	Sloped				Sloped with holes				Sloped with ribs			
					$d_s$ (cm)	$W_s$ (cm)	$L_u$ (cm)	$L_d$ (cm)	$d_s$ (cm)	$W_s$ (cm)	$L_u$ (cm)	$L_d$ (cm)	$d_s$ (cm)	$W_s$ (cm)	$L_u$ (cm)	$L_d$ (cm)
0.33	7.97	32.0	16.0	23.0	4.1	26	11.4	11.5	5.02	30.6	13.4	13.5	3.6	26	11.3	11.2
0.31	6.9	31.5	15.4	21.5	3.4	24.3	10.5	11	4.31	26.8	13.0	12.9	3.12	23.2	10.5	9.6
0.26	6.3	29.0	15.0	16.5	2.61	23.8	10.0	10.3	3.9	25.3	11.2	11.4	1.9	23.2	9.4	8.8
0.23	4.9	28.0	12.0	15.0	1.8	23.6	10.0	9.8	3.1	25	10.8	10.8	1.5	22.9	8.0	8.0
0.20	4.2	21.5	9.4	13.5	1.45	22.6	9.0	9.0	2.69	24	10.5	10.5	1.34	20	8.0	7.5
0.18	3.3	16.7	9.0	11.0	1.31	20	9.0	7.0	2.34	22.2	10.0	10.0	0.91	19.2	0.0	0.0

Table 3. Percentage influence for the relative dimensions of scour hole comparing with the case of no collars.

Relative dimension Shape	$d_s/b\%$			$W_s/b\%$			$L_u/b\%$			$L_d/b\%$		
	Sloped	Sloped with holes	Sloped with ribs	Sloped	Sloped with holes	Sloped with ribs	Sloped	Sloped with holes	Sloped with ribs	Sloped	Sloped with holes	Sloped with ribs
Fr												
0.33	48	37	56	19	4	19	29	16	29	50	41	51
0.31	50	37	55	23	9	26	32	16	32	49	40	55
0.26	59	38	69	18	13	20	33	25	37	38	31	47
0.23	64	37	69	16	11	18	17	10	33	35	28	47
0.20	65	35	68	-5	-12	7	4	-6	15	33	22	44
0.18	60	28	72	-20	-33	-15	0	-10	100	36	9	100

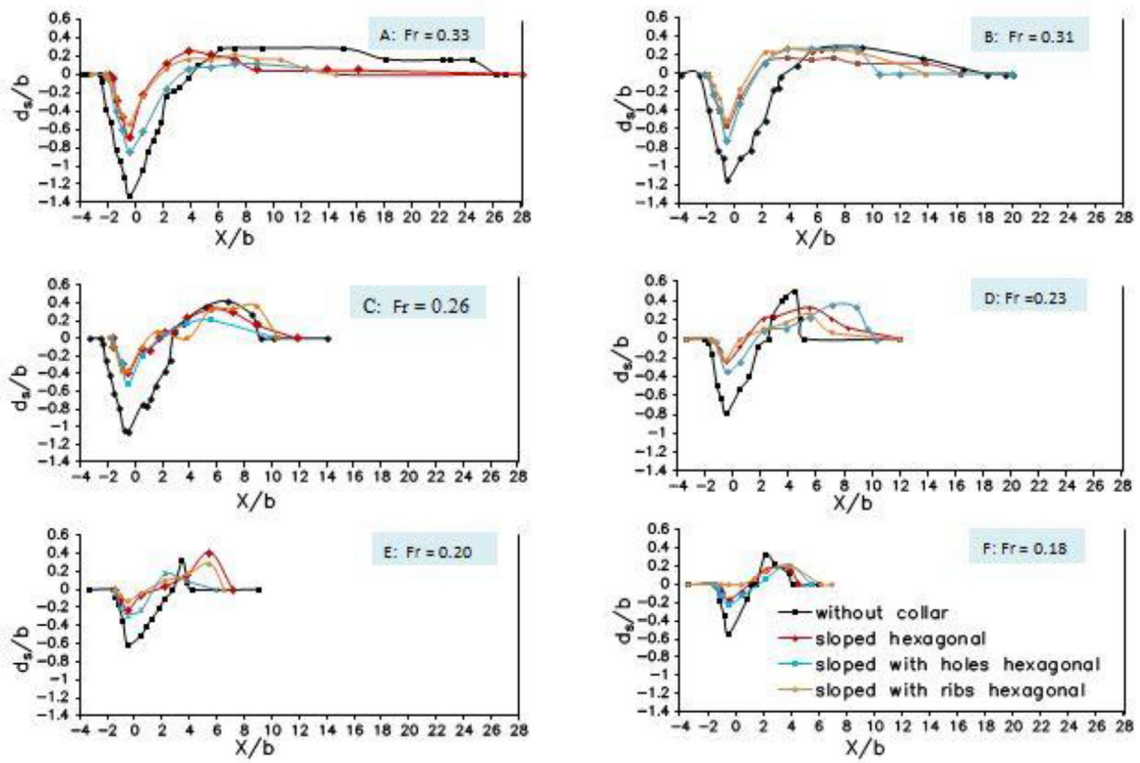


Fig. 6. Longitudinal profiles of scour holes for pier without a collar and hexagonal collars at ( $Fr = 0.33$  to  $0.18$ ).

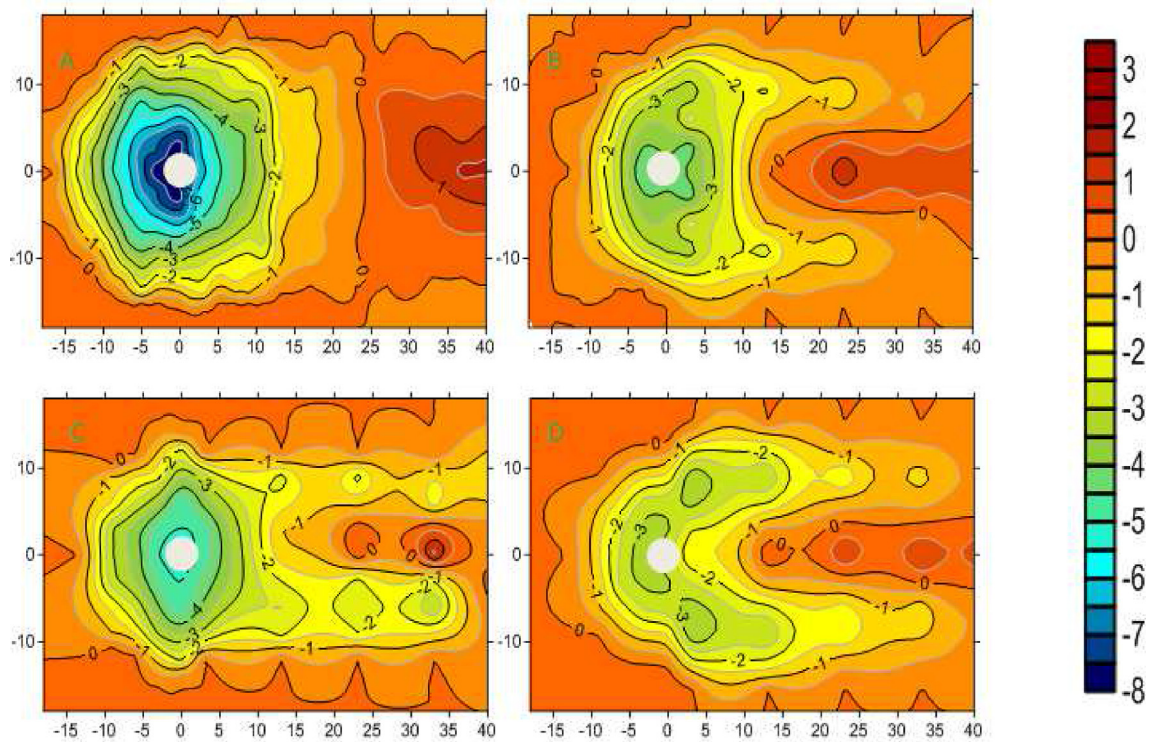


Fig. 7. Scour contour maps at equilibrium stages around the circular pier, the pier without collar (A), sloped (B), sloped with holes (C), sloped with ribs (D), at  $Fr = 0.33$ .



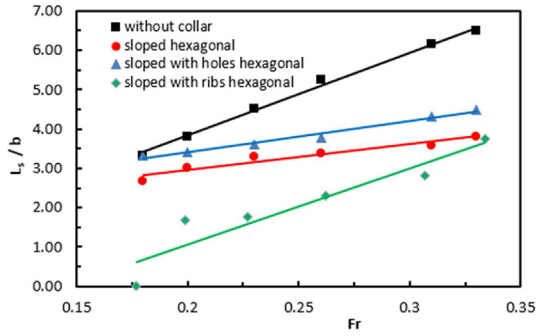


Fig. 8. Relationship between  $(L_s/b)$  and Froude numbers  $(Fr)$  for pier without collar and pier with hexagonal collars.

scour of all cases can be obtained by dividing the values of Table 2 by the diameter of the pier ( $b = 6.0$  cm). The percentage values of influence of the considered models compared with the case of the pier without collar are listed in Table 3, these considered values can be calculated by  $\% = \left( \frac{R_w - R_h}{R_w} \right)$ .

Where;  $R_w$  are the relative dimensions of considered values for scour holes at the pier without a collar.  $R_h$  are the relative dimensions of considered values for scour hole at the pier with hexagonal collars.

#### 4.1. The impact of Collar's shape and froude number on scour topography and longitudinal profiles

Fig. 6 shows a comparison between the longitudinal scour hole profile at the pier without collar and various hexagonal collars for each Froude number at the equilibrium time. Fig. 7 illustrates scour contour map at equilibrium stages around circular pier for Froude Number equals 0.33. The  $L_s/b$  values represented in Fig. 8 are obtained by adding the values of  $\left( \frac{L_w}{b} + \frac{L_d}{b} \right)$ . It is clear from this figure that by increasing Froude number from 0.18 to 0.33, all relative scour hole lengths for the pier without a collar are increased with a rate from  $(L_s/b = 3.33–6.50)$ . The lengths of the unprotected scour holes are longer than those for all cases of pier with hexagonal collar. Relative scour hole length at sloped, sloped with holes, and sloped with ribs hexagonal collars are increased with a rate from  $(2.67–3.81)$ ,  $(3.31–4.48)$ , and  $(0–3.74)$ , respectively for the same values of Froude numbers. For all Froude numbers, sloped with ribs hexagonal collar gives the lowest value of the relative length of scour hole. The trend of the results of the sloped collar with ribs has the same trend as the pier rate without collar (nearly parallel).

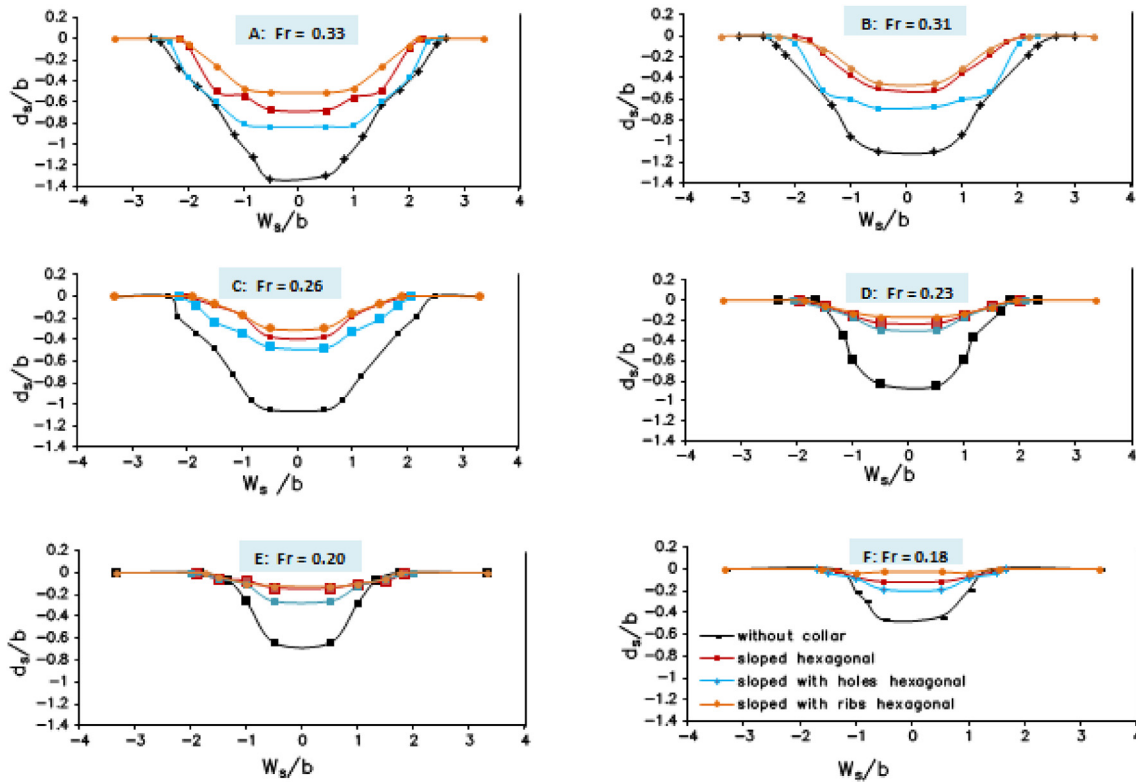


Fig. 9. Transversal-section profile of scour hole for pier without collar and various shapes of hexagonal collar at  $(Fr = 0.33$  to  $0.18)$ .

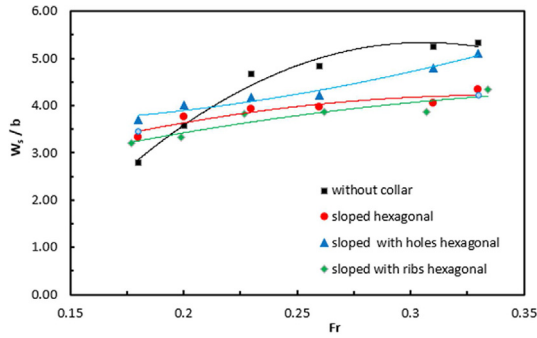


Fig. 10. Relationship between  $(W_s/b)$  and  $(Fr)$  for the considered cases.

For the pier without collar, the length of the scour hole behind the pier is longer than its extension in the front. The differences between the lengths of the scour hole in front and behind the pier with various hexagonal collars are small.

Where: A positive sign (+) indicates positive action (decreasing the relative dimensions of scour hole). A negative sign (–) indicates negative action (increasing the relative dimensions of scour hole comparing with pier without collar).

#### 4.2. The effect of Collar's shape and froude number on transversal scour profiles

For the same considered Froude numbers, Fig. 9 depicts the transversal-section of maximum width for the pier without collar and hexagonal collars at the equilibrium time. For Fig. 10 it's clear that the relative width of scour for pier without a collar is increased from  $(W_s/b = 2.78–5.33)$  with increasing the Froude numbers from  $(0.18–0.33)$ . The relative scour widths for the pier with sloped, sloped with holes, and sloped with ribs, respectively are increased with a rate of  $(3.33–4.33)$ ,  $(3.7–5.1)$  and  $(3.2–4.33)$  with the above-mentioned values of Froude number. The relative width of scour for various hexagonal collars is wider than the relative

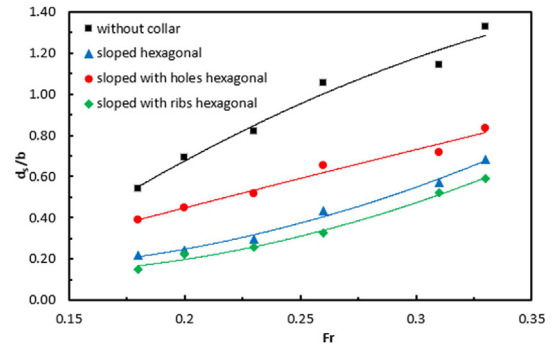


Fig. 11. Relationship between relative scour depth  $(d_s/b)$  and Froude numbers  $(Fr)$  for pier without collar and hexagonal collars.

width for pier without collar at lower Froude numbers  $(0.18$  and  $0.20)$ . With increasing Froude numbers  $(0.23–0.33)$ . The widths of the unprotected scour hole become wider than those in the cases of pier with collar. Lower erosive flow power and narrower hole dimensions result from the edges of the hexagonal collar dispersing the downflow and separating it from the horseshoe vortices.

#### 4.3. The impact of Collar's shape and froude numbers on maximum scour depth

To clear the influence of the proposed model in scour depth, Photo 3 and Fig. 11 depict the observed scour hole characteristics measured at the pier's center for the position of a pier with hexagonal collars and without collar. Fig. 12 clears the percentage effect (reduction) for the relative scour depth of scour hole compared with the case of no collars. The figure represented that the scour holes dimensions increased with increasing the Froude number. Pier without collar gave the maximum scour depth for all Froude numbers. At all Froude numbers, the sloped with ribs hexagonal collar provided the least scour depth with a reduction

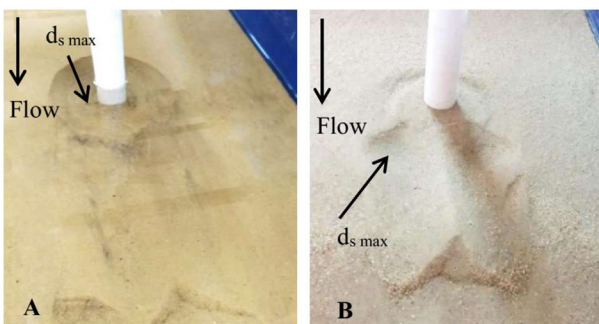


Photo 3. (A) Shape of scour hole for pier without collar and (B) Shape of scour hole for pier with hexagonal collar (sloped with ribs).

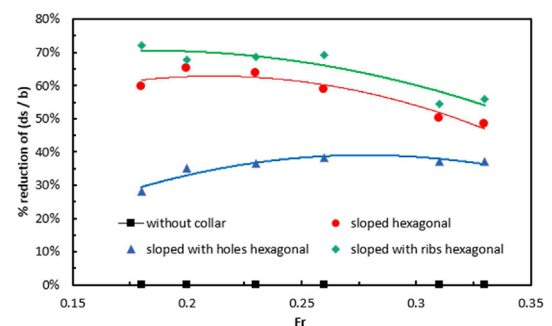


Fig. 12. % Reduction of relative scour depth  $(d_s/b)$  comparing with the case with no collar for Froude Numbers  $(Fr)$ .

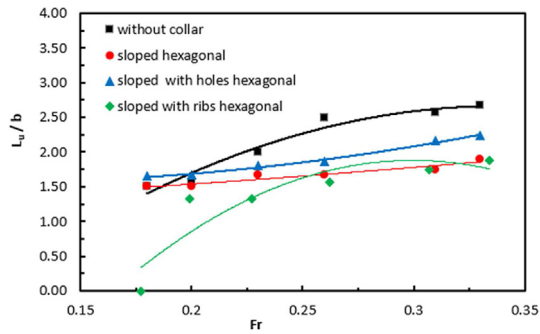


Fig. 13. Relationship between  $(L_u/b)$  and Froude number ( $Fr$ ) for pier without collar and pier with hexagonal collars.

percent of 56%. Sloped with holes hexagonal gave the large scour depth, compared with other collars, but still smaller than that of the pier with no collar. For the proposed hexagonal collars, maximum scour depths are shifted to the downstream direction, where the collar is separated between the downflow and horseshoe vortices, so that the maximum scour depths decrease. Maximum scour depths for the pier with no collars case are used as a reference for the obtained other maximum scour depth results from the cases of hexagonal collars.

#### 4.4. Up and down stream dimensions of scour hole

For each run, the horizontal dimensions of the scour hole are measured to determine the relative relevance of each parameter on scour hole. For the same discharge, the correlations between Froude numbers and different horizontal dimensions of the scour hole around the bridge pier are plotted. Figs. 13 and 14 exhibit the differences in the relative upstream and downstream lengths of scour hole ( $L_u/b$ ), ( $L_d/b$ ), and Froude numbers ( $Fr$ ). Table 3 shows the percentage effect of relative upstream and downstream scour lengths compared with the case of no collars. The results showed that sloped hexagonal

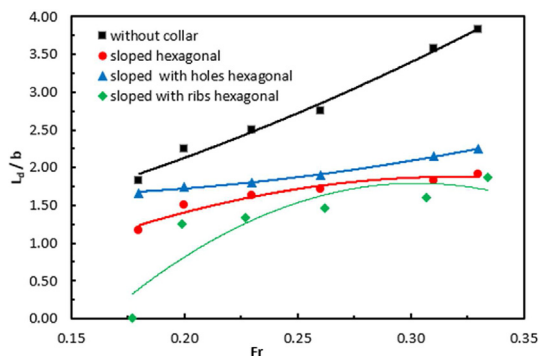


Fig. 14. Relationship between  $(L_d/b)$  and Froude number ( $Fr$ ) for pier without collar and pier with hexagonal collars.

with ribs gave the greatest reduction in the dimensions of scour hole compared with the others shapes where ribs dissipating more the impinging downflow. Fig. 15 shows the influence percentage for relative dimensions of scour hole comparing with the case of no collars.

## 5. Derivation of maximum scour parameters

Most well-known and commonly used equations primarily focus on estimating the maximum scour depth at unprotected piers. In this study, experimental data were utilized to develop empirical formulas that not only predict the maximum scour depth but also address other important scour dimensions, including scour width and scour lengths around the pier. Moreover, a novel coefficient of collar model effect ( $K_m$ ) has been proposed to enhance the applicability of the suggested formulas in predicting scour dimensions at both unprotected and protected (collared) piers. Furthermore, the innovative coefficient,  $K_m$ , can be integrated into commonly used scour prediction methods to broaden their applicability, encompassing both unprotected and protected piers.

The MATLAB Nonlinear Regression was applied to the laboratory results, resulting in the empirical formulas of the relative scour hole dimensions, the innovative collar model impact coefficients, and the determination coefficients displayed in Table 4.

Fig. 16 shows the relationship between the laboratory-observed relative scour depth, width, and lengths those predicted by the developed formulas (Table 4). The applicability of the relations, as shown, reveals significant correlations between measured and computed values for all Froude numbers,  $Fr$ , and the novel model coefficients,  $K_m$ , at outstanding determination coefficients,  $R^2$ .

Furthermore, the confidence in the created relationships in Table 4 for estimating scour dimensions was tested using the commonly used statistical indicators and their acknowledged boundaries after Najafzadeh and Barani (2011), Drudi et al. (2019) and Abdulkathum et al. (2023), which are listed below. The MAE (mean absolute error) represents the closeness of estimated to observed scour dimension values, and the RMSE (root mean square error) is frequently used as a prediction error metric. When MAE and RMSE approach zero, they indicate the prediction method is capable. A prediction method's accuracy is measured by its MAPE (mean absolute percentage error). According to the literature classification, predicting accuracy is excellent when  $MAPE \leq 10\%$ ,

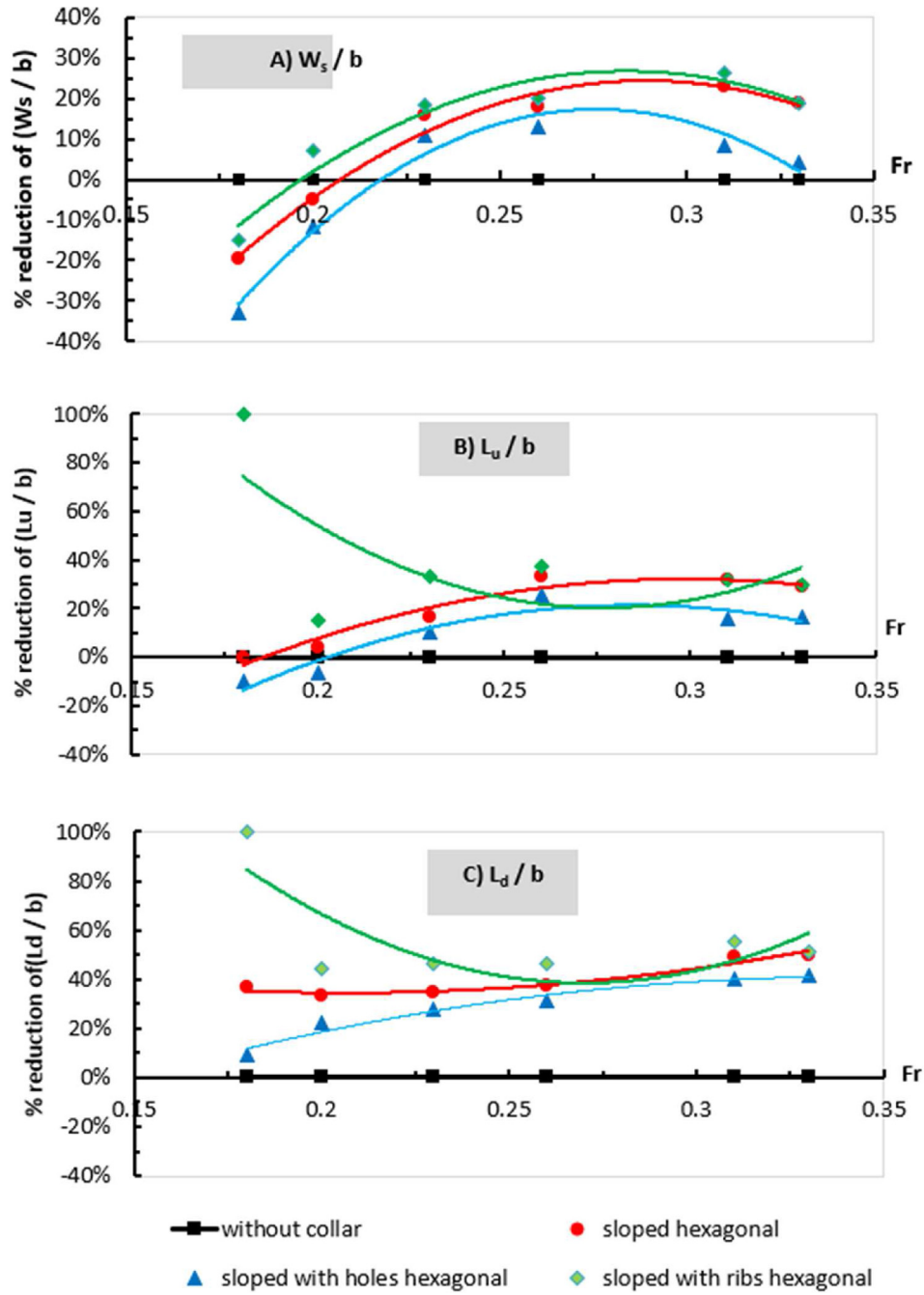


Fig. 15. % Influence of relative dimensions of scour hole comparing with the case of the pier without collar for Froude Numbers ( $Fr$ ).

Table 4. Relations for predicting scour dimensions and innovative coefficients,  $K_m$ .

Formulas	Sloped hexagonal collar	Sloped with holes hexagonal collar	Sloped with ribs hexagonal collar	$R^2$	Eqn. no.
$\frac{d_s}{b} = 6.5890 Fr^{1.4343} * K_m$	0.4560	0.6351	0.3914	0.972	(9)
$\frac{W_s}{b} = 9.6026 Fr^{0.5539} * K_m$	0.8705	0.9723	0.8365	0.850	(10)
$\frac{L_u}{b} = 5.5872 Fr^{0.6869} * K_m$	0.7633	0.8746	0.7014	0.887	(11)
$\frac{L_d}{b} = 9.6012 Fr^{0.8861} * K_m$	0.5700	0.6697	0.5041	0.953	(12)

\*Consider that for an unprotected pier case (without collar):  $K_m = 1.0$ .



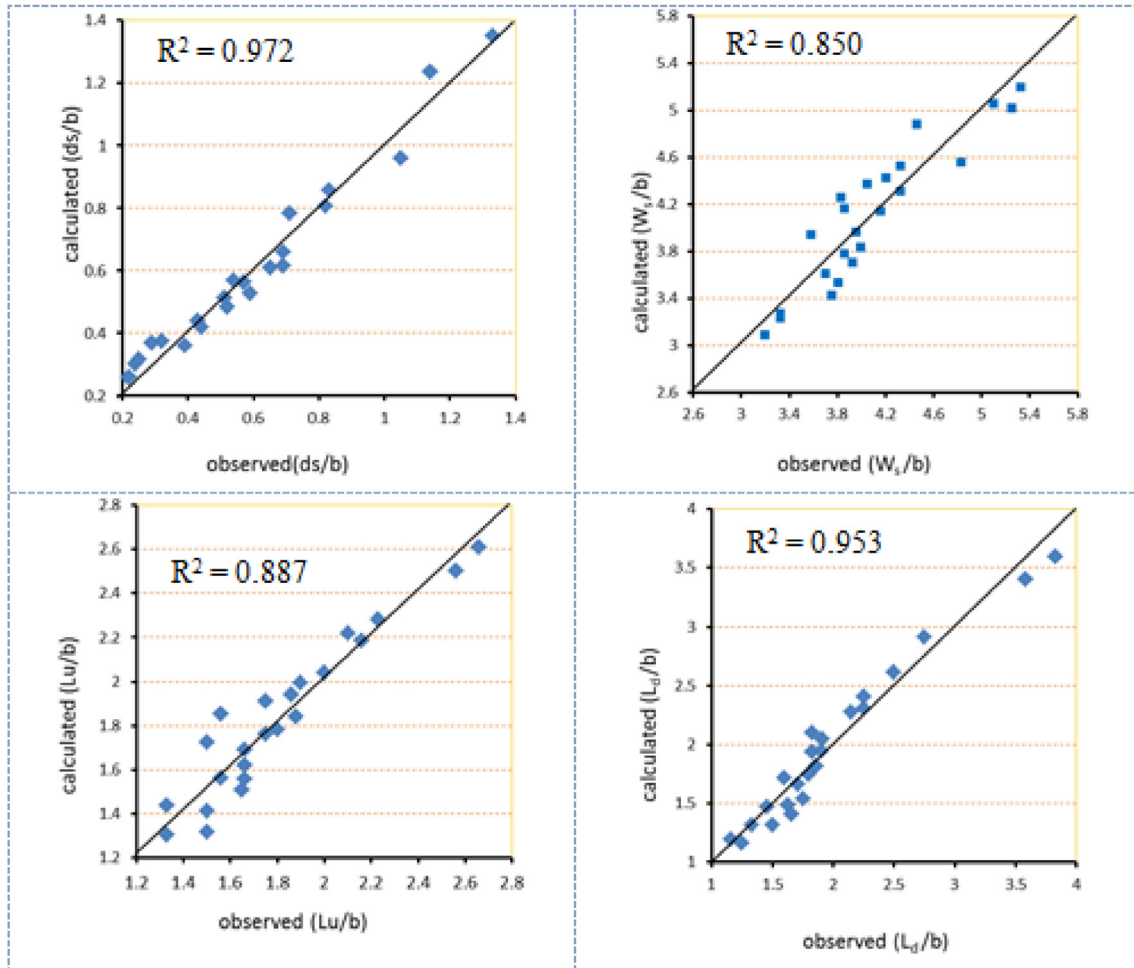


Fig. 16. Comparison between experimental and computed results.

good when  $10\% < \text{MAPE} \leq 20\%$ , acceptable when  $20\% < \text{MAPE} \leq 50\%$ , and unacceptable when  $\text{MAPE} > 50\%$ .

---


$$\text{The mean absolute error (MAE)} = \frac{1}{n} * \sum_{i=1}^N \left| \frac{d_s \text{measured}}{b} - \frac{d_s \text{calculated}}{b} \right| \quad (13)$$

$$\text{The root mean square error (RMSE)} = \sqrt{\frac{\sum_{i=1}^N \left| \frac{d_s \text{measured}}{b} - \frac{d_s \text{calculated}}{b} \right|^2}{N}} \quad (14)$$

$$\text{The mean absolute percentage error (MAPE)} = \frac{100}{N} \sum_{i=1}^N \frac{\left| \frac{d_s \text{measured}}{b} - \frac{d_s \text{calculated}}{b} \right|}{\frac{d_s \text{measured}}{b}} \quad (15)$$

Table 5. Statistical indicators.

Equation	R <sup>2</sup>	MAE	RMSE	MAPE
$\frac{d_s}{b} = 6.5890 Fr^{1.4343} * K_m$	0.972	0.044	0.051	3.232
$\frac{W_s}{b} = 9.6026 Fr^{0.5539} * K_m$	0.850	0.183	0.179	4.534
$\frac{L_u}{b} = 5.5872 Fr^{0.6869} * K_m$	0.887	0.083	0.109	4.873
$\frac{L_d}{b} = 9.6012 Fr^{0.8861} * K_m$	0.953	0.108	0.139	5.280

Table 6. Collected data from the previous studies and present study.

Parameter Investigator	b (m)	D (m)	Fr (-)	d <sub>s</sub> /b (-)
Moncada-M et al. (Moncada et al., 2009)	0.073	2b	0.2–0.32	0.3–0.99
Negm et al. (Negm et al., 2009)	0.03	5b	0.2–0.55	0.0–0.2
Safaei et al. (Safaei et al., 2021)	0.03	3b	0.19–0.30	0.4–0.90
Raeisi, Ghomeshi (Raeisi and Ghomeshi, 2022)	0.04	4b	0.26–0.37	0.35–0.72
Present study, Eqn. (9)	0.06	3b	0.18–0.33	0.15–0.6

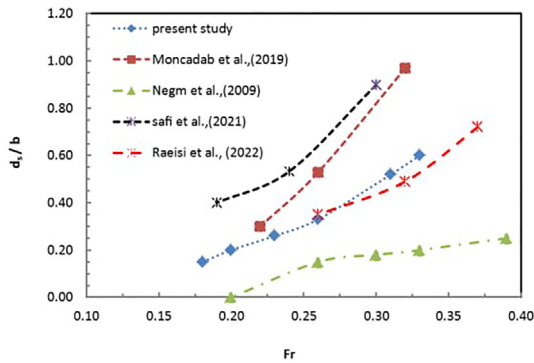


Fig. 17. Comparative analysis between present study with other research using scour countermeasures.

Where: N is the number of observations (N = 24).

Table 5 displays the obtained values of the used metrics based on the above-mentioned literature classification of the indicators. As can be observed, all statistical values for indexes demonstrate the outstanding accuracy of formulas 9–12, which

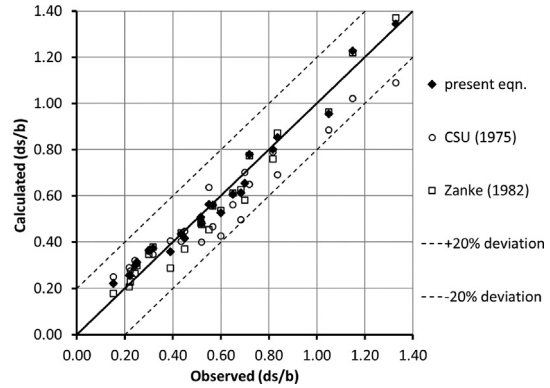


Fig. 18. Validation of the modified and suggested formulas.

provide good predictions of scour hole dimensions in the range of tested Froude numbers under clear-water scour conditions.

### 6. Comparative analysis between present study with other research using scour countermeasures (collar)

Table 6 and Fig. 17 show the comparison between the present and previous studies. The results indicated that the current study gives satisfactory results compared with the other ones.

The developed novel,  $K_m$ , is used to modify two of the well-known scour depth prediction equations, namely: Zanke (1982) and CSU1975 (Richardson and Davis, 2001) equations. The coefficient of collar model effect is used as multiplication factor in the original equations as in equations (16) and (17). Fig. 18 shows the well prediction of the new developed formula (Eqn. 9) as well as the modified equations of CSU1975 and Zanke1982 for both unprotected and collared pier under clear-water scour conditions. As shown, around 100% and 75% of the estimated scour depths were found to be within 20% and 15% prediction errors, respectively, when the  $K_m$  coefficient implemented.

$$\text{Modified CSU 1975: } \frac{d_s}{b} = 2.20 (Fr)^{0.43} \left(\frac{h}{b}\right)^{0.65} \cdot K_m \quad (16)$$

$$\text{Modified Zanke1982: } \frac{d_s}{b} = \begin{cases} \left(\frac{V}{V_{cr}} \omega - 1\right) \cdot K_m, \frac{V}{V_{cr}} < 1 \\ \left[ \frac{\omega}{\left(\frac{V_{cr}}{V} + \frac{V_{cr}^2}{V^2} + \frac{V_{cr}^3}{V^3}\right)^{0.50}} - 1 \right] \cdot K_m, \frac{V}{V_{cr}} > 1 \end{cases} \quad (17)$$

Where:  $\omega$  = the effective velocity Increase due to turbulence

## 7. Conclusions

In this paper, experimental study using collar models were used to investigate the effect of using hexagonal collars with different shapes on reducing scour around a cylindrical bridge pier. In general, the results revealed that, using collars proved to be more effective in reducing scour around bridge piers. The main conclusions drawn from this study are as follows:

- (1) Scour hole dimensions increased with increasing Froude numbers.
- (2) Using hexagonal collars shift the maximum scour depth to the downstream direction away from the pier.
- (3) Transversal-sectional profile of scour indicates that, the relative widths of the scour hole for hexagonal collars, at Froude numbers  $>0.2$  are smaller than the relative widths of scour around pier without collar. At Froude numbers  $\leq 0.2$  the relative width is larger than that of the case of no collar.
- (4) Sloped with ribs hexagonal collar has the ability to minimize maximum scour depth around pier with about 56%.
- (5) Sloped with ribs hexagonal collar could minimize maximum width, upstream and downstream lengths of scour around pier by 19%, 29% and 51%, respectively.
- (6) Sloped with ribs hexagonal collar is the most effective shape in reducing scour around pier comparing with the other hexagonal collars.
- (7) Amount of scour around sloped with holes hexagonal collar is much more than the other collars.
- (8) Several regression relationships are developed to simulate the experimental results of maximum relative scour depth, width, and length. There are very minor differences between the experimental and computed results.

## 8. Notation

The following symbols are used in this paper:

- $b$  = Diameter of pier (cm),  
 $B$  = Width of flume (cm),  
 $D$  = Diameter of collar (cm),  
 $d_s$  = Maximum depth of scour hole (cm),  
 $d_{50}$  and  $\sigma$  = Sediment median diameter (mm) and Geometric standard deviation.  
 $Fr$  = Froude Number,  
 $g$  = Gravitational acceleration ( $m/s^2$ ),

- $h$  = Approach flow depth (cm),  
 $K_m$  = Effect coefficient of collar's model,  
 $L$ : The considered dimension of the scour hole (cm),  
 $L_u$  = Upstream length of scour hole (cm),  
 $L_d$  = Downstream length of scour hole (cm),  
 $R$  = Correlation coefficient,  
 $T$  = Required time to reach the equilibrium scour hole(s),  
 $U_{cr}^*$  = Critical shear velocity for the sediment,  
 $V$  = Mean flow velocity (m/s),  
 $V_{cr}$  = Critical mean approach velocity (m/s),  
 $W_s$  = Maximum width of scour hole (cm),  
 $\nu$  = Water dynamic viscosity, and  
 $\rho$  and  $\rho_s$  = Water and sediment densities, respectively

## Credit statement

**Heba Kassem:** Conceptualization, Methodology, Experimentation, Writing-original draft.

**A.A. El-Masry:** Conceptualization, Methodology, Supervision, Review.

**Reda Diab:** Conceptualization, Methodology, Experimentation, Formal analysis, Writing-review & editing.

## Funding statement

No financial support was received.

## Conflicts of interest

The author declared that there are no potential conflicts of interest with respect to the research authorship or publication of this article.

## References

- Abdulkathum, S., Al-Shaikhli, H.I., Al-Abody, A.A., Hashim, T.M., 2023. Statistical analysis approaches in scour depth of Bridge Piers. *Civ. Eng. J* 9, 143–153. <https://doi.org/10.28991/CEJ-2023-09-01-011>.
- Bestawy, A., Eltahawy, T., Alsaluli, A., Almaliki, A., Alqurashi, M., 2020. Reduction of local scour around a bridge pier by using different shapes of pier slots and collars. *Water Supply* 20, 1006–1015. <https://doi.org/10.2166/ws.2020.022>.
- Breusers, H., Nicollet, G., Shen, H., 1977. Local scour around cylindrical piers. *J. Hydraul. Res.* 15, 211–252.
- Chiew, Melville, 1987. Local scour around bridge piers. *J. Hydraul. Res.* 25, 15–26. <https://doi.org/10.1080/00221688709499285>.
- Diab, R., Link, O., Zanke, U., 2010. Geometry of developing and equilibrium scour holes at bridge piers in gravel. *Can. J. Civ. Eng.* 37, 544–552. <https://doi.org/10.1139/109-176>.
- Drudi, K.C., Drudi, R., Martins, G., Antonio, G.C., Jtc, Leite, 2019. Statistical model for heating value of municipal solid waste in Brazil based on gravimetric composition. *Waste Manag.* 87, 782–790.

- Gumgum, F., Guney, M.S., 2020. Time dependent live-bed scour around circular piers under flood waves. *Period. Polytech. Civ. Eng.* 64, 65–72. <https://doi.org/10.3311/PPci.14664>.
- Gupta, L.K., Pandey, M., Raj, P.A., Pu, J.H., 2023. Scour reduction around bridge pier using the airfoil-shaped collar. *Hydrology* 10, 77.
- Helmi, A.M., Shehata, A.H., Abbas, M.M., El-manadely, M.S., 2019. Experimental assessment of circular collar effect on local scour around single cylindrical pier and numerical investigation of flow structure. *Al-Azhar Univ Civil Eng Res Mag* 41, 3.
- Melville, Chiew, 1999. Time scale for local scour at Bridge Piers. *J. Hydraul. Eng.* 125, 59–65. [https://doi.org/10.1061/\(asce\)0733-9429\(1999\)125:1\(59\)](https://doi.org/10.1061/(asce)0733-9429(1999)125:1(59)).
- Melville, Coleman, 2000. In: Coleman, B.W. M.a.S.E. (Ed.), *Bridge Scour*. Water Resources Publications, LLC.
- Moncada, -M.A., Aguirre-Pe, J., Bolivar, J., Flores, E., 2009. Scour protection of circular bridge piers with collars and slots. *J. Hydraul. Res.* 47, 119–126.
- Najafzadeh, M., Barani, G.-A., 2011. Comparison of group method of data handling based genetic programming and back propagation systems to predict scour depth around bridge piers. *Sci. Iran.* 18, 1207–1213.
- Negm, A.M., Moustafa, G.M., Abdalla, Y.M., Fathy, A.A., 2009. Optimal shape of collar to minimize local scour around bridge piers. *Proc IWTC* 13, 12–15.
- Pandey, M., Azamathulla, H.M., Chaudhuri, S., Pu, J.H., Pourshahbaz, H., 2020. Reduction of time-dependent scour around piers using collars. *Ocean Eng.* 213, 107692. <https://doi.org/10.1016/j.oceaneng.2020.107692>.
- Raeisi, N., Ghomeshi, M., 2022. A laboratory study of the effect of asymmetric-lattice collar shape and placement on scour depth and flow pattern around a bridge pier. *Water Supply* 22, 734–748. <https://doi.org/10.2166/ws.2021.239>.
- Raudkivi, A., Etema, R., 1983. Clearwater scour at cylindrical piers. *J. Hydraul. Eng.* 109. [https://doi.org/10.1061/\(ASCE\)0733-9429\(1983\)109:3\(338\)](https://doi.org/10.1061/(ASCE)0733-9429(1983)109:3(338)).
- Richardson, E.V., Davis, S.R., 2001. *Evaluating Scour at Bridges*, fourth ed.
- Safaei, A., Solimani Babarsad, M., Agha Majidi, R., Eftekhari, P., 2021. Experimental study effect of the flexible collar on bridge pier scouring depth. *Irrigation Sci Eng* 44, 53–66. <https://doi.org/10.22055/JISE.2021.37936.1982>.
- Tafarojnoruz, A., Gaudio, R., Dey, S., 2010. Flow-altering countermeasures against scour at bridge piers: a review. *J. Hydraul. Res.* 48, 441–452. <https://doi.org/10.1080/00221686.2010.491645>.
- Zanke, U., 1982. Scours at piles in steady flow and under the influence of waves ('Kolke am Pfeiler in richtungskonstanter Stroemung und unter Welleneinfluss', in German). *Mitteilungen des Franzius-Instituts für Wasserbau-und Küsteningenieurwesen der Universität Hannover*, Heft 54, 381–416.